Temperature dependence of an AlInP 63Ni betavoltaic cell

Article (Accepted Version)

Temperature dependence of an AlInP ^{63}Ni betavoltaic cell

Silvia Butera[1,*)], Grammatiki Lioliou[1], Andrey B. Krysa[2], Anna M. Barnett[1]

[1]Semiconductor Materials and Device Laboratory, School of Engineering and Informatics, University of Sussex, Brighton, BN1 9QT, UK.
[2]EPSRC National Centre for III-V Technologies, University of Sheffield, Mappin Street, Sheffield, S1 3JD, UK.

Abstract. In this paper the performance of an $Al_{0.52}In_{0.48}P$ ^{63}Ni radioisotope cell is reported over the temperature range -20 °C to 140 °C. A 400 μm diameter p^+-i-n^+ (2 μm i-layer) $Al_{0.52}In_{0.48}P$ mesa photodiode was used as conversion device in a novel betavoltaic cell. Dark current measurements on the $Al_{0.52}In_{0.48}P$ detector showed that the saturation current increased increasing the temperature, while the ideality factor decreased. The effects of the temperature on the key cell parameters were studied in detail showing that the open circuit voltage, the maximum output power and the internal conversion efficiency decreased when the temperature was increased. At -20 °C, an open circuit voltage and a maximum output power of 0.52 V and 0.28 pW, respectively, were measured.

Keywords: $Al_{0.52}In_{0.48}P$, betavoltaic, semiconductors, photodiode

I. INTRODUCTION

Radioisotope microbatteries are potentially attractive options for systems needing small amounts (pW to μW) of power over extended periods of time (10 – 100+ years). In radioisotope betavoltaic batteries, beta particles are emitted during nuclear decay of a radioisotope and absorbed by a semiconductor converter device generating an electrical energy that may be useful in emerging technologies such as microelectromechanical system technologies (MEMS) [1]. Implantable medical devices in biomedical applications [3], in particular, could take advantages in using this type of power supply since these batteries could insure a high life-quality in the

* Corresponding author. Electronic mail: S.Butera@sussex.ac.uk.

patients requiring implantation, as there is no need of recharge or replacement.

The use of the beta emitter ^{63}Ni has received research attention for use in betavoltaics because of its ability to produce relatively high output powers with minimal risk for the semiconductor conversion device (endpoint energy of 66 keV). Different wide bandgap semiconductors, including GaAs, SiC, GaN and diamond, have been previously coupled to ^{63}Ni radioisotope beta particle sources and investigated as novel betavoltaic microbattery prototypes. Wang et al. [4] demonstrated a ^{63}Ni-GaAs microbattery with 0.075% conversion efficiency at 20 °C; while Butera et al. [5] proved a ^{63}Ni-GaAs cell with internal conversion efficiencies of 11% and 22% at 20 °C and at -20 °C, respectively. Chandrashekhar et al. reported a ^{63}Ni-SiC microbattery with at least 6% efficiency [6], whilst Eiting et al. a ^{33}P-SiC microbattery with 4.5% efficiency [7] at room temperature. Cheng et al. [8] investigated a high open circuit voltage (1.64 V) ^{63}Ni-GaN beta-voltaic microbattery with a conversion efficiency of 0.98% at room temperature; while Bormashov et al. [9] proved a ^{63}Ni-diamond beta-voltaic microbattery with conversion efficiencies as high as 0.6% at room temperature.

The choice of a wide bandgap semiconductor as the converter material is desirable since they can be used in harsh environment condition with reduced likelihood of radiation damage from the integrated radioisotope or from external radiation sources. Moreover, they can operate at elevated temperatures without cooling systems and wider bandgaps are expected to result in high conversion efficiencies [5].

$Al_{0.52}In_{0.48}P$ is a wide bandgap semiconductor (indirect bandgap of 2.31 eV [2]) which has received much attention for use in optoelectronics. However, it is only recently that it has been demonstrated for use in the detection of higher energy radiations e.g. for photon counting X-ray spectroscopy [10, 11]. $Al_{0.52}In_{0.48}P$ is nearly lattice matched with GaAs and the crystalline quality of the nearly lattice matched $Al_{0.52}In_{0.48}P$ can be very high in comparison to III-V nitrides, IV and II-VI compounds of a similar bandgap. The doping in $Al_{0.52}In_{0.48}P$ is also easier to control than in some II-VI semiconductors. Consequently, $Al_{0.52}In_{0.48}P$ is a potentially important material for radioisotope microbatteries.

In this paper an $Al_{0.52}In_{0.48}P$ ^{63}Ni radioisotope betavoltaic cell is demonstrated for the first time. The effect of temperature on the key cell parameters were studied and are presented over the temperature range -20 °C to 140 °C.

II. DEVICE STRUCTURE

The p^+-i-n^+ $Al_{0.52}In_{0.48}P$ structure was grown, using metalorganic vapour phase epitaxy (MOVPE), on a commercial (100) n-GaAs:Si substrate with a misorientation of 10 degrees towards <111>A to suppress the CuPt-like ordered phase. The p^+-i-n^+ $Al_{0.52}In_{0.48}P$ structure consisted of a 0.2 μm Zn-doped p-type $Al_{0.52}In_{0.48}P$ layer, a 2 μm undoped $Al_{0.52}In_{0.48}P$ layer, and 0.1 μm Si-doped n-type $Al_{0.52}In_{0.48}P$ layer. The doping concentrations of the $Al_{0.52}In_{0.48}P$ p^+ and n^+ layers were 5×10^{17} cm^{-3} and 2×10^{18} cm^{-3}, respectively. A GaAs layer, 0.01 μm thick, was grown on top of the p^+-i-n^+ $Al_{0.52}In_{0.48}P$ structure to facilitate the top metal contact deposition. An Ohmic top contact consisting of 20 nm of Ti and 200 nm of Au was evaporated on the p-side of the structure, whilst an Ohmic rear contact consisting of 20 nm of InGe and 200 nm of Au was evaporated onto the rear of the substrate. The device layers, their relative thicknesses and materials are summarised in Table I. After growth, the wafer was patterned and etched using 1:1:1 H_3PO_4:H_2O_2:H_2O solution followed by 10 s in 1:8:80 H_2SO_4: H_2O_2: H_2O solution. A 400 μm diameter unpassivated p^+-i-n^+ $Al_{0.52}In_{0.48}P$ mesa photodiode, with top Ohmic contact covered 33% of its surface, was used in the developed betavoltaic cell. The 400 μm diameter unpassivated p^+-i-n^+ $Al_{0.52}In_{0.48}P$ mesa photodiode was illuminated by a ^{63}Ni radioactive source (activity 185 MBq; electron energies up to 66 keV); the source was positioned as close as experimentally possible (3mm) to the top of the device such to minimize the attenuations of the electrons in the dry nitrogen environment of the temperature test chamber where the cell was placed for the study.

Table I. Layer details of the $Al_{0.52}In_{0.48}P$ photodiode

Layer	**Material**	**Thickness (μm)**	**Dopant**	**Dopant Type**	**Doping density (cm^{-3})**
1	Ti	0.02			
2	Au	0.2			
3	GaAs	0.01	Zn	p^+	1×10^{19}
4	$Al_{0.52}In_{0.48}P$	0.2	Zn	p^+	5×10^{17}
5	$Al_{0.52}In_{0.48}P$	2	undoped		

6	$Al_{0.52}In_{0.48}P$	0.1	Si	n^+	2×10^{18}
7	Substrate n^+ GaAs				
8	Au	0.2			
9	InGe	0.02			

The Monte Carlo computer modelling package CASINO (version 3.3) [12, 13] was used to simulate the interaction of the beta electrons in the $Al_{0.52}In_{0.48}P$ ^{63}Ni radioisotope betavoltaic cell; the amount of beta energy absorbed in the $Al_{0.52}In_{0.48}P$ i-layer was particularly studied. In the simulations, 4000 beta particles, of energies between 1 keV and 66 keV, were simulated as emitted from the source and incident on the p^+-side of the $Al_{0.52}In_{0.48}P$ epilayer. The simulations showed that beta particles with energies below 22 keV did not reach the $Al_{0.52}In_{0.48}P$ i-layer primarily because of the attenuation of the particles' energies in the protective inactive Ni overlayer of the radioisotope beta particle source used. Attenuation in the top metal contact (covering 33% of the diode's face) and in the GaAs dead layer was a secondary effect, as well as the attenuation through the p^+ layer of the $Al_{0.52}In_{0.48}P$ device. Beta electrons with energy $\geq$ 22 keV deposited part of their energy in the i-layer. Simulations suggested that the electrons at 39 keV were the electrons that deposited the highest percentage of their energy in the i-layer (17%): beta particles with energies < 39 keV lost most of their energy above the i-layer, whilst the beta particles with energies > 39 keV easily passed through the 2 μm thick i-layer depositing there only a small percentage of their energy (e.g. only 8% of the energy of the 66 keV was absorbed in the i-layer). The current cell design is, therefore, optimised for absorption of the 39 keV electrons. It should be noted that the emission of beta electron with energies of 17 keV is the most probable from ^{63}Ni the emission probability, by comparison the relative emission probability of beta electrons with energies of 39 keV is 0.5 [14]. Future changes in the system design, such as the use of a ^{63}Ni radioisotope beta source without a protective inactive Ni overlayer and a thicker $Al_{0.52}In_{0.48}P$ i-layer and a thinner p^+-layer, will allow the absorption of electrons in a wider range of energies so that a bigger percentage of the energy released by the source will be deposited in the i-layer. The attenuation of the beta particles in the dry nitrogen gap (3 mm) was also investigated with CASINO and found to be negligible compared to the other losses.

III. RESULTS AND DISCUSSION

The $Al_{0.52}In_{0.48}P$ ^{63}Ni radioisotope betavoltaic cell was studied in the temperature range 140 °C to -20 °C using TAS Micro MT climatic cabinet to achieve and maintain the temperature investigated. Dry nitrogen was constantly flowing inside the test chamber to control the humidity of the atmosphere where the cell was tested (relative humidity < 5%). A Keithley 6487 picoammeter/voltage source was used to study the cell performance. Forward bias measurements in dark conditions and under the illumination of the ^{63}Ni radioisotope beta source were conducted at biases between 0 V and 1 V in 0.01 V increments. The uncertainty associated with the current readings was 0.3% of their values plus 400 fA, while the uncertainty associated with the applied biases was 0.1% of their values plus 1 mV [15].

Dark current characteristics as a function of forward bias at different temperatures for the $Al_{0.52}In_{0.48}P$ ^{63}Ni radioisotope betavoltaic cell are shown in Figure 1. At high temperatures, the dark currents through the devices increased due to the greater thermal energy available.

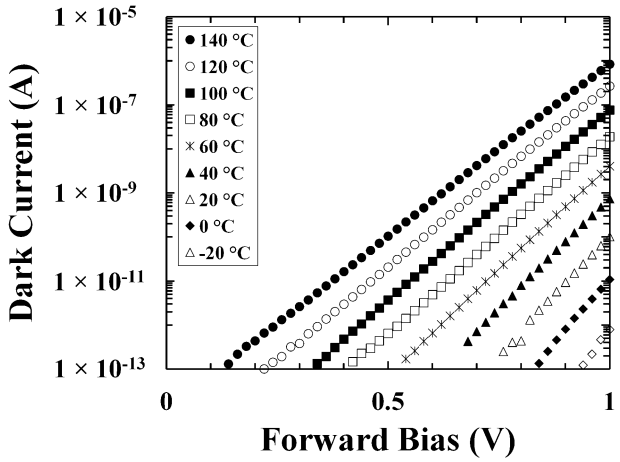

Figure 1. Dark current as a function of applied forward bias for the $Al_{0.52}In_{0.48}P$ ^{63}Ni radioisotope betavoltaic cell. The temperatures studied were 140 °C (filled circles), 120 °C (empty circles), 100 °C (filled squares), 80 °C (empty squares), 60 °C (crosses), 40 °C(filled triangles), 20 °C (empty triangles), 0 °C (filled rhombuses) and -20 °C (empty rhombuses).

At increased forward bias, a greater electric field is applied across the photodiode's depletion region resulting in higher dark current at each temperature. Equation 1 shows the relationship between the dark current and the applied bias for a simple p-n diode.

$$I = I_0 \exp\left\{ qV / nkT \right\} \quad (1)$$

where I_0 is the saturation current, q is the electric charge, n is the ideality factor, k is the Boltzmann constant and T is the temperature [16]. At each temperature, the values of I_0 and n for the $Al_{0.52}In_{0.48}P$ photodiode were experimentally estimated by performing a linear least squares fit of the natural logarithm of the measured dark current data as a function of applied forward bias: equation (1) was linearised as Ln I = A + BV, with A = Ln I_0 and B = q(nkT)$^{-1}$, and used linear least square fitting. Figure 2 shows the logarithm of the measured saturation current (left axis, filled circles) and the ideality factor (right axis, crosses) as functions of temperature, respectively.

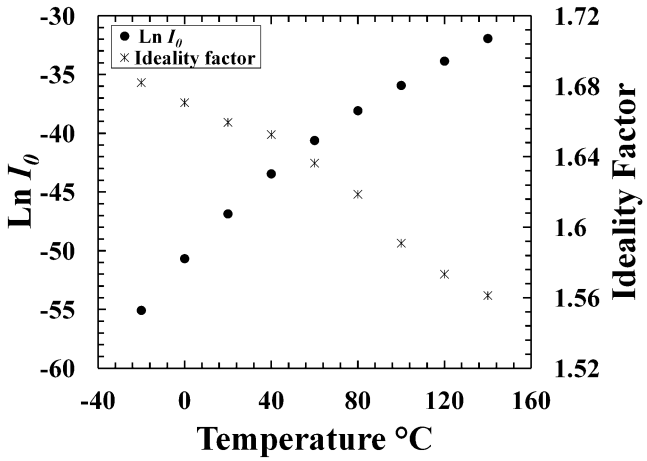

Figure 2. The logarithm of the saturation current (left axis, filled circles) and the ideality factor (right axis, crosses) as a function of temperature for the $Al_{0.52}In_{0.48}P$ device.

In accordance with ref. [17], the magnitude of the natural logarithm of the saturation current increased at decreased temperatures. The observed increase was 23.13 ± 0.19 (corresponding to an increase in saturation current, I_0, of 0.013 pA) between 140 °C and -20 °C. This was in remarkable agreement with the expected increase of 20.50 (corresponding to an increase in saturation current, I_0, of 0.008 pA). The expected increase was calculated using the simple assumption that the temperature dependence of the natural logarithm of the saturation current was proportional to $E_g/2kT$ [18]. In the same temperature range, a change in ideality factor was also observed. Since the ideality factor was > 1.5 at every temperature, it can be concluded that the generation-recombination mechanism was dominant over the diffusion mechanism. The lower

value of ideality factor observed at higher temperature (1.561 ± 0.003 at 140 °C vs 1.682 ± 0.011 at -20 °C) may be attributed to the increased contribution of the diffusion current at increased temperature [16]. A similar dependence of ideality factor as a function of temperature has been previously observed in other semiconductors, e.g. GaAs [19].

Figure 3 shows the illuminated current characteristics as a function of forward bias at different temperatures for the $Al_{0.52}In_{0.48}P$ ^{63}Ni radioisotope betavoltaic cell. The open circuit voltage (V_{OC}) and the short circuit current (I_{SC}) were extrapolated as the interception points of the curves with the horizontal and vertical axes, respectively.

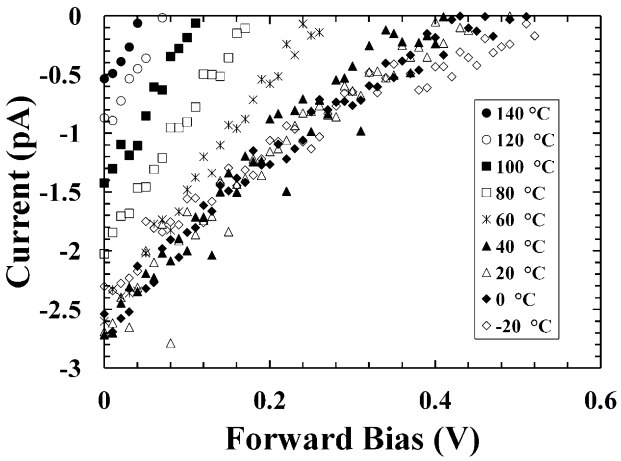

Figure 3. Current as a function of applied forward bias for the $Al_{0.52}In_{0.48}P$ ^{63}Ni cell. The temperatures studied were 140 °C (filled circles), 120 °C (empty circles), 100 °C (filled squares), 80 °C (empty squares), 60 °C (crosses), 40 °C (filled triangles), 20 °C (empty triangles), 0 °C (filled rhombuses) and -20 °C (empty rhombuses).

At temperatures above 40 °C, the current through the $Al_{0.52}In_{0.48}P$ device increased when the temperature was decreased; a different trend was instead observed at temperatures below 40 °C. In the temperature range between 40 °C and -20 °C, the measured current characteristics were noisy and overlapped each other indicating that saturation effects from beta particle induced conduction became dominant over the thermal mechanism (scattering), the significance of which was greater at higher temperatures as would be expected. The beta electrons, losing energy through the $Al_{0.52}In_{0.48}P$ structure, generated electron-hole pairs along their trajectories that decreased the resistivity in that region [16]. A similar mechanism has been previously observed in GaAs ^{63}Ni cell [5].

The open circuit voltage (V_{OC}) and the short circuit current (I_{SC}) as a function of temperature for the $Al_{0.52}In_{0.48}P$ ^{63}Ni radioisotope betavoltaic cell are shown in Figure 4 and Figure 5, respectively.

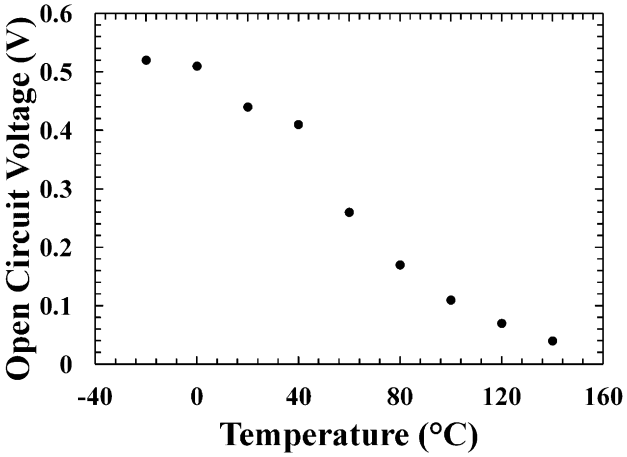

Figure 4. Open circuit voltage as a function of temperature for the $Al_{0.52}In_{0.48}P$ ^{63}Ni radioisotope beta cell.

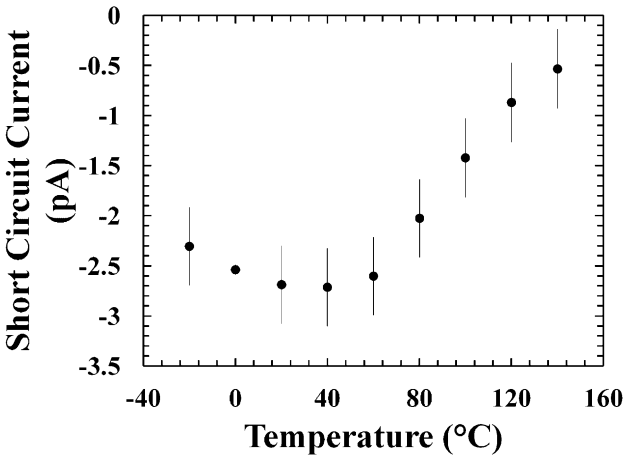

Figure 5. Short circuit current as a function of temperature for the $Al_{0.52}In_{0.48}P$ ^{63}Ni radioisotope beta cell.

The open circuit voltage (V_{OC}) decreased with increased temperature. The V_{OC} values obtained for the $Al_{0.52}In_{0.48}P$ ^{63}Ni radioisotope betavoltaic cell were lower than the values reported in ref. [17] for an $Al_{0.52}In_{0.48}P$ ^{55}Fe radioisotope X-ray photovoltaic microbattery where a similar $Al_{0.52}In_{0.48}P$ structure was used. This could be due to the higher carrier density in $Al_{0.52}In_{0.48}P$ when it was illuminated with beta electrons compared with X-ray photons: the beta electrons creating an increased amount of electron-hole pairs along their trajectories decreased the material resistivity,

consequently lower open circuit voltage values were observed in comparison to ref. [17]. The conductive mechanism and its effect were more evident at low temperatures since it was dominant over the thermal mechanism. A similar behaviour for V_{OC} was observed in GaAs ^{63}Ni cell [5]. The exact mechanism by which the V_{OC} appears to saturate at low temperatures is not currently conclusively known, however X-ray illuminated measurements with a similar structure did not show a saturation in V_{OC} [17], thus it is hypothesised that the beta illumination mechanism used in the present paper was responsible for this effect possibly as a consequence of the conductive mechanism's dominance at these low temperatures. The conductive mechanism also influenced the short circuit current (I_{SC}) values observed: the short circuit current magnitude increased with decreasing temperature from 140 °C to 40° C, it reached a saturation value of 2.7 pA between 40 °C and -20 °C. The slight decrease in *Isc* observed for temperatures < 20 °C was unexpected and its mechanism is unclear, however, the apparent change recorded is within the experimental uncertainties.

The $Al_{0.52}In_{0.48}P$ ^{63}Ni radioisotope betavoltaic cell output power was calculated as $P = IV$. Increasing the applied forward bias, the cell output power increased to a maximum (P_m) and then decreased, as shown in Figure 6. At temperatures below 40 °C the power characteristics were noisy and overlapped each other as a consequence of the current results shown in Figure 3. Figure 7 (left axis, filled circles) shows the magnitude of the measured maximum output power as a function of temperature. The internal conversion efficiency of the betavoltaic cell was also calculated dividing the experimental maximum output power by the maximum power (P_{th}). P_{th} was calculated using equation 2

$$P_{th} = \sum_{i=0}^{endpoint=66} \frac{A}{2} Em_i \frac{A_{Ni}}{A_{AlInP}} QE_i \frac{i}{w_{AlInP}} 1.6 \times 10^{-19} \qquad (2)$$

where A is the activity of the ^{63}Ni radioactive source (185 MBq), Em_i the emission probability of an electron of energy i [14], A_{Ni} area of the ^{63}Ni radioactive source (49 mm^2), A_{AlInP} area of the $Al_{0.52}In_{0.48}P$ detector (0.13 mm^2), QE_i the percentage of each electron energy absorbed in the $Al_{0.52}In_{0.48}P$ mesa device (calculated using CASINO software), ω_{AlInP} the $Al_{0.52}In_{0.48}P$ electron-hole pair creation energy (5.34 eV [20]). In equation 2 the activity of the ^{63}Ni radioactive source was halved because we assumed that half of the electrons were lost since they were emitted up. P_{th} was found to be 4.3

pW.

Figure 7 (right axis, empty squares) shows the cell internal conversion efficiency as a function of temperature.

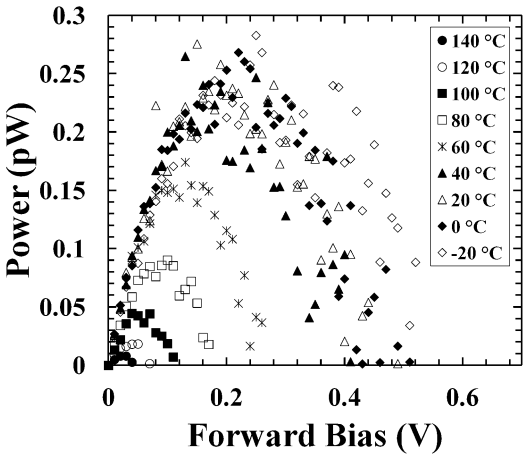

Figure 6. $Al_{0.52}In_{0.48}P$ ^{63}Ni radioisotope cell output power as a function of applied forward bias at 140 °C (filled circles), 120 °C (empty circles), 100 °C (filled squares), 80 °C (empty squares), 60 °C (crosses), 40 °C (filled triangles), 20 °C (empty triangles), 0 °C (filled rhombuses) and -20 °C (empty rhombuses).

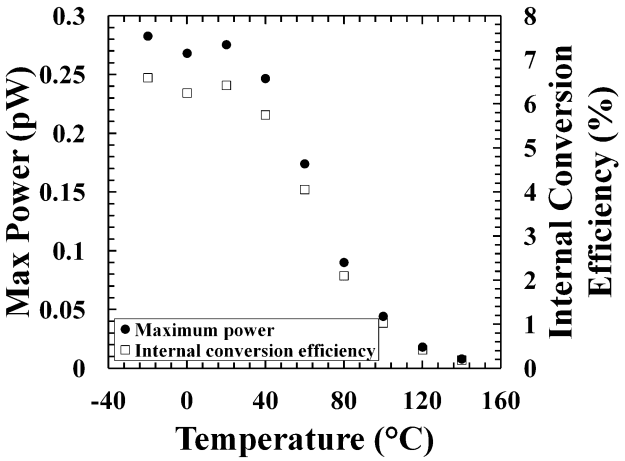

Figure 7. The experimental maximum power (left axis, filled circles) and the internal conversion efficiency (right axis, empty squares) as a function of temperature for the $Al_{0.52}In_{0.48}P$ device.

In Figure 7, the magnitude of the maximum output power increased decreasing the temperature, reaching a saturation value of 0.28 pW, corresponding to 0.11 μW/Ci, at temperatures < 40 °C. The behaviour observed can be explained taking in consideration the dependence of the maximum output power with respect to the open

circuit voltage [16]. At each temperature, the maximum output power values were lower than the ones observed using a similar $Al_{0.52}In_{0.48}P$ converter device and an ^{55}Fe radioisotope X-ray source [17]. The use of the beta electrons decreased the $Al_{0.52}In_{0.48}P$ resistivity, as a consequence of conductive mechanism, resulting in an underestimation of the maximum output power values. At -20 °C, maximum output power of 0.28 pW was observed for the $Al_{0.52}In_{0.48}P$ ^{63}Ni radioisotope betavoltaic cell, whilst 0.62 pW was extracted from a single cell of the $Al_{0.52}In_{0.48}P$ ^{55}Fe radioisotope X-ray photovoltaic microbattery [17]. The underestimation of the maximum output power resulted in lower cell internal efficiency with respect to ref. [17]. At -20 °C, a internal conversion efficiency of 6.6% was achieved for the $Al_{0.52}In_{0.48}P$ ^{63}Ni radioisotope betavoltaic, while 22% was reported by for the $Al_{0.52}In_{0.48}P$ ^{55}Fe radioisotope X-ray photovoltaic microbattery [17].

Improvements in the cell system design, such as the use of a radioisotope beta particle source without a protective inactive Ni overlayer and the optimization of the radioisotope beta particle source to converter device geometry, will improve the next generation of $Al_{0.52}In_{0.48}P$ ^{63}Ni radioisotope betavoltaic cell. Maximising the number of electrons collected by the $Al_{0.52}In_{0.48}P$ converter device, as well as the fraction of their energy deposited in the i-layer, will increase the maximum cell output power. Currently only 0.13% of the beta particles emitted by the ^{63}Ni radioisotope source reached the $Al_{0.52}In_{0.48}P$ device. The number of electrons per second emitted in any direction by the beta source was estimated knowing the ^{63}Ni radioactive source's activity (185 MBq) and emission probabilities [14]; it was found that 5.6×10^7 electrons per second are emitted by the ^{63}Ni radioactive source. Of these 5.6×10^7 electrons per second, only half are emitted in the direction of the device (we assumed that half of the electrons were lost because emitted up). The number of electron per second on the device (7.2×10^4 s^{-1}) was estimated knowing the number of electrons per second emitted by the source towards the device (2.8×10^7 s^{-1}) and the geometry of the source and detector. The ratio between the area of the device (0.13 mm^2) and the area of the radioactive ^{63}Ni source (49 mm^2) was calculated to be 0.0026.

IV. CONCLUSIONS

In this paper for the first time the performance of an $Al_{0.52}In_{0.48}P$ ^{63}Ni radioisotope cell are reported. Preliminary dark current measurements showed that the $Al_{0.52}In_{0.48}P$ saturation current increased as the temperature was increased, while the ideality factor decreased. Under illumination from the ^{63}Ni radioisotope, the open circuit voltage, the maximum output power and the internal conversion efficiency of the $Al_{0.52}In_{0.48}P$ betavoltaic cell decreased with increased temperatures. A maximum output power of 0.28 pW (corresponding to 0.11 μW/Ci) and an internal conversion efficiency of 6.6% were observed, respectively, at -20 °C. A better microbattery system design that improves the beta particle collection (currently only 0.13% of the beta particles reached the $Al_{0.52}In_{0.48}P$ i-layer) could increase the power extracted from the betavoltaic cell. Conductive mechanisms, particularly evident at low temperatures, seemed to compromise the cell performance: despite the high energy of the beta particles with respect to the X-ray photons, the maximum output power of the $Al_{0.52}In_{0.48}P$ ^{63}Ni radioisotope cell was lower than $Al_{0.52}In_{0.48}P$ ^{55}Fe radioisotope X-ray photovoltaic microbattery [17].

Acknowledgment

This work was supported by STFC grant ST/M002772/1 (University of Sussex, A. M. B., PI). The authors are grateful to R. J. Airey and S. Kumar at the EPSRC National Centre for III-V Technologies for device fabrication. G. Lioliou acknowledges funding received from University of Sussex in the form of a PhD scholarship.

References

[1] K. E. Bower, Y. A. Barbanel, Y. G. Shreter and G. W. Bohnert, Polymers, phosporors, and voltaics for radioisotope microbatteries, CRC Press LLC, Boca Raton, 2002.

[2] J. S. Cheong, J. S. Ong, J. S. Ng, A. B. Krysa and J. P. R. David, AlInP SAM-APD as a Blue-Green Detector, *IEEE J. Sel. Topics Quantum Electron.* **20**, 142-146 (2014).

[3] G. Kotzar, M. Freas, P. Abel, A. Fleischman, S. Roy, C. Zorman, J. M. Moran and J. Melzak, Evaluation of MEMS materials of construction for implantable medical devices, *Biomaterials* **23**, 2737-2750 (2002).

[4] H. Wang, X-B. Tang, Y-P. Liu, Z-H. Xu, M. Liu and D. Chen, Temperature effect on betavoltaic microbatteries based on Si and GaAs under ^{63}Ni and ^{147}Pm irradiation, *Nucl. Instrum. Methods Phys. Res., Sect. B* **359**, 36-43 (2015).

[5] S. Butera, G. Lioliou and A. M. Barnett, Gallium Arsenide ^{63}Ni betavoltaic cell, Submitted to *Semicond. Sci. Tech.* (2016).

[6] M. Chandrashekhar, C. I. Thomas, H. Li, M. G. Spencer and A. Lal, Demonstration of a 4H SiC betavoltaic cell, *Appl. Phys. Lett.* **88**, 033506 (2006).

[7] C. J. Eiting, V. Krishnamoorthy, S. Rodgers and T. George, Demonstration of a radiation resistant, high efficiency SiC betavoltaic, *Appl. Phys. Lett.* **88**, 064101**(**2006).

[8] Z. Cheng, X. Chen, H. San, Z. Feng and B. Liu, A high open-circuit voltage gallium nitride betavoltaic microbattery, *J. Micromech. Microeng.* **22**, 074011 **(**2012).

[9] V. Bormashov, S. Troschiev, A. Volkov, S. Tarelkin, E. Korostylev, A. Golovanov, M. Kuznetsov, D. Teteruk, N. Kornilov and S. Terentiev, Development of nuclear microbattery prototype based on Schottky barrier diamond diodes, *Phys. Status Solidi A* **212**, 2539-2547 (2015).

[10] A. Auckloo, J. S. Cheong, X. Meng, C. H. Tan, J. S. Ng, A. B. Krysa, R. C. Tozer and J. P. R. David, $Al_{0.52}In_{0.48}P$ avalanche photodiodes for soft X-ray spectroscopy, *J. Inst.* **11**, P03021(2016).

[11] S. Butera, G. Lioliou, A. B. Krysa and A. M. Barnett, Characterisation of $Al_{0.52}In_{0.48}P$ mesa pin photodiodes for X-ray photon counting spectroscopy, *J. Appl. Phys.* **120**, 024502 (2016).

[12] P. Hovington, D. Drouin and R. Gauvin, CASINO: A new Monte Carlo code in C language for electron beam interaction—Part I: Description of the program, *Scanning* **19**, 1-14 (1997).

[13] D. Drouin, P. Hovington and R. Gauvin, CASINO: A new monte carlo code in C language for electron beam interactions—part II: Tabulated values of the mott cross section, *Scanning* **19**, (1997) 20-28.

[14] I. L. Preiss, R. W. Fink and B. L. Robinson, The beta spectrum of carrier-free Ni^{63}, *J. Inorg. Nucl. Chem.* **4**, 233-236 (1957).

[15] Keithley Instruments Inc, Model 6487 Picoammeter/Voltage Source Reference Manual, 6487-901-01 Rev B, Cleveland, 2011.

[16] S. M. Sze and K. K. Ng, Physics of semiconductor devices, Third Ed., John Wiley & Sons, New Jersey, 2007.

[17] S. Butera, G. Lioliou, A. B. Krysa and A. M. Barnett, $Al_{0.52}In_{0.48}P$ ^{55}Fe X-ray-photovoltaic battery, *J. Phys. D*: *Appl. Phys*. **49**, 355601 (2016).

[18] M. Chandrashekhar, R. Duggirala, M. G. Spencer and A. Lal, 4HSiC betavoltaic powered temperature transducer, *J. Appl. Phys.* **91**, 053511**(**2007).

[19] G. Lioliou, X. Meng, J. S. Ng and A. M. Barnett, Temperature dependent characterization of gallium arsenide **X**-ray mesa pin photodiodes, *J. Appl. Phys* **119**, 124507 (2016).

[20] S. Butera, G. Lioliou, A. B. Krysa and A. M. Barnett, Electron-hole pair creation energy in $Al_{0.52}In_{0.48}P$, Submitted to *Sci. Rep* (2016).